

Molecular Docking Studies of Halogenated Bicyclo[4.2.0] Inositols with SARS-CoV-2 Proteins

Ebrar Nur Şahin¹ , Abdullah Karanfil² , Ertan Şahin¹ , Latif Kelebekli² 

¹Department of Chemistry, Faculty of Sciences, Ataturk University, Erzurum 25240, Turkey

²Department of Chemistry, Faculty of Sciences and Arts, Ordu University, Ordu 52200, Turkey

Geliş Tarihi / Received Date: 05.11.2021

Kabul Tarihi / Accepted Date: 09.12.2021

Abstract

Cyclic sulfate is the precursor compound that can adapt well to the binding sites of the docked proteins of SARS-CoV-2. Cyclic sulfate showed very strong molecular interactions for the 6lu7, 6zb5 and 6vww proteins of SARS-CoV-2, with binding energies of -7.33, -7.29 and -7.29 kcal mol⁻¹, respectively. Besides, acetate showed very strong molecular interactions with -7.45 kcal mol⁻¹ for the 6lu7 protein of SARS-CoV-2. Therefore, according to our results, cyclic sulfate and acetate should be investigated as a promising drug candidate for the treatment of COVID-19.

Keywords: molecular docking, RdRp, Mpro, SGp, inositol

Halojenli Bisiklo[4.2.0] İnositollerin SARS-CoV-2 Proteinleri ile Moleküler Doking Çalışmaları

Özet

Siklik sülfat, SARS-CoV-2'nin kenetlenmiş proteinlerinin bağlanma bölgelerine iyi uyum sağlayabilen öncü bileşiktir. Siklik Sülfat, SARS-CoV-2'nin 6lu7, 6zb5 ve 6vww proteinleri için sırasıyla -7.33, -7.29 ve -7.29 kcal mol⁻¹ 'lük bağlanma enerjileriyle çok güçlü moleküler etkileşimler gösterdi. Ayrıca asetat, SARS-CoV-2'nin 6lu7 proteini için -7.45 kcal mol⁻¹ ile çok güçlü moleküler etkileşimler gösterdi. Bu nedenle sonuçlarımıza göre siklik sülfat ve asetat, COVID-19 tedavisi için umut verici bir ilaç adayı olarak araştırılmalıdır.

Anahtar Kelimeler: moleküler doking, RdRp, Mpro, SGp, inositol

Introduction

Inositols which have a hexahydroxycyclohexane skeleton are the important subclass of cyclitol family. Their structures are analogous to those of replacing endo-oxygen atom with a methylene group in monosaccharides (1). This replacement provides some advantages to the molecule. Unlike carbohydrates, the absence of the acetal moiety (2) in inositols (Figure 1) protects them from hydrolysis and makes them chemically and biologically resistant (Zanardi et al., 2002). Due to their structural resemblance to sugars many polyhydroxylated alkaloids form an important family of glycosidase inhibitors (López et al., 2008). Bicyclic polyhydroxylated alkaloids such as (+)-castanospermine (3) and (-)-swainsonine and their chemically modified derivatives are also effective antiviral, antitumor and immunomodulatory agents (Wang et al. 2010) and identified as naturally occurring glycosidase inhibitors in plants and microorganisms (Kelebekli et al., 2005). We have previously performed molecular insertion studies on AChE and BuChE enzymes for enzyme inhibition for type 2 diabetes patients. In the previous study, it has been shown that cyclic sulfate is more active against AChE, BuChE and α -glucosidase with the calculated binding energies of -8.22, -7.58 and -6.59 kcal.mol⁻¹, respectively, compared to the galantamine and acarbose standard from which the binding energy is calculated (Şahin et al., 2022).

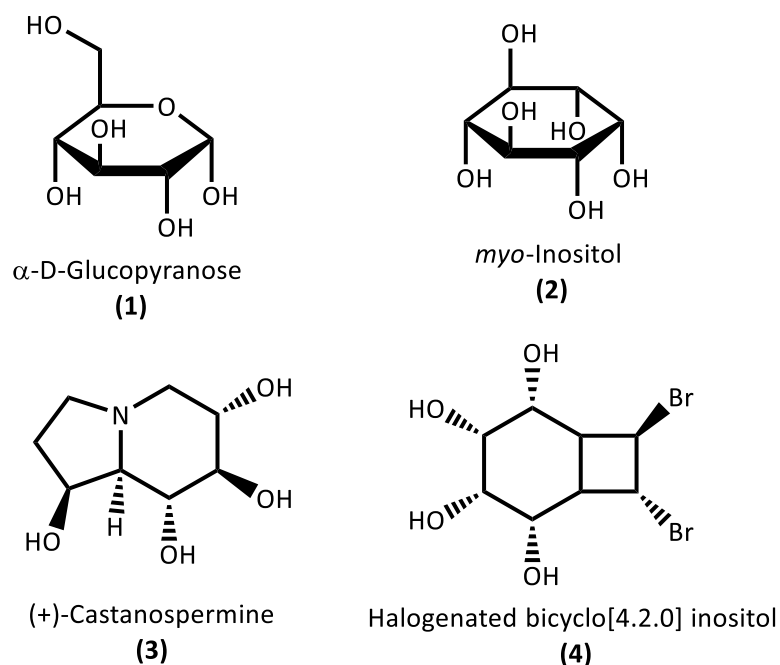


Figure 1. Some Carbasugar Derivatives

The most abundant isomer of inositols is the *myo*-inositol (2). *Myo*-inositol (2) is ingested with food mostly from fruits, beans, grains, and nuts (Kamenov & Gateva, 2020). *Myo*-Inositol (2) proved to reduce Interleukin-6 (IL-6) levels in a few conditions and to alleviate the inflammatory cascade, while being devoid of any major side effects (Bizzarri et al., 2020; Lagana et al., 2020). *Myo*-inositol (2) supplementation may represent a possible alternative therapy to counteract the hyper-immune activation induced by COVID-19 involving activation of the IL-6 cascade. Also, *myo*-inositol (2) can stimulate pulmonary surfactant production, thereby reducing inflammatory processes (Espinola et al., 2021). Scyllo-inositol, one of many isomers of 1,2,3,4,5,6-cyclohexanehexol, has been shown to have promising potential as a therapeutic for Alzheimer's disease by directly interacting with the amyloid β ($A\beta$) peptide to inhibit $A\beta$ 42 fiber formation. A single fluoro substitution and 1,4-dimethylation of scyllo-inositol provide compounds that remain effective in inhibiting $A\beta$ 42 fiber formation (Sun et al., 2008). Due to the important biological activities of inositols, many research groups focus on the synthesis of bicyclo and/or halogenated derivatives (Aksu et al., 2020; Kelebekli & Atli, 2019; Kelebekli & Kaplan, 2017).

The new human coronavirus, called severe acute respiratory syndrome coronavirus 2 (SARS-CoV-2), first appeared in Wuhan, China, in late 2019. This virus spread rapidly around the world, causing the respiratory illness called coronavirus disease 2019 (COVID-19). Given the multiple threats and disturbances posed by the pandemic, scientists around the world are racing to understand SARS-CoV-2 and explore its pathophysiology to find potential treatments and effective therapeutic drug candidates. Pandemic COVID-19 infections have spread all over the world. There is no effective treatment for this disease. Viral RNA-dependent RNA polymerase (RdRp) catalyzes the replication of RNA from RNA and the main protease (Mpro) is involved in processing polyproteins translated from the RNA of SARS-CoV-2 and therefore these two enzymes are potent candidates for targeting by anti-viral drugs. Although various therapeutic agents have been evaluated for the treatment of 2019 coronavirus disease (Covid-19), no antiviral agents have yet been shown to be effective. Small molecules such as lopinavir and favipiravir significantly inhibit the activity of Mpro and RdRp in vitro. Studies have shown that structurally modified lopinavir, favipiravir, and other similar compounds can inhibit the COVID-19 major protease (Mpro) and RNA-dependent RNA polymerase (RdRp) (Rafi et al. 2020). In this study, lopinavir was chosen to bind to the main protease and structurally similar compounds and favipiravir to target RNA-dependent RNA polymerase. In addition, remdesivir was chosen as the drug for Spike/ACE2. Seeing the worldwide health crisis, our goal was to find a suitable drug candidate that could target SARS-CoV-2. Remdesivir, an inhibitor of the viral RNA-dependent, RNA polymerase with in vitro inhibitory activity against SARS-CoV-1 and the Middle East respiratory syndrome (MERS-CoV) (Agostini et al., 2018; Brown et al., 2019; Sheahan et al., 2017), was identified early as a promising therapeutic candidate for Covid-19 because of its ability to inhibit SARS-CoV-2 in vitro (Wang et al 2020). In addition, in nonhuman primate studies, remdesivir initiated 12 hours after inoculation with MERS-CoV (de Wit et al., 2013; de Wit et al., 2020) reduced lung virus levels and lung damage. As of October 22, 2020, remdesivir, an antiviral agent, is the only drug approved for treatment of COVID-19 (de Wit et al., 2020). The approved drugs used were Azithromycin, Ritonavir, Lopinavir, Oseltamivir, Ivermectin and Heparin, which are emerging as promising agents in the fight against COVID-19 (Arouche et al., 2021).

Favipiravir, also known as T-705, a purine nucleic acid analogue, is one of the antiviral candidates evaluated in several clinical trials. It is an experimental chemical and was first created by Japanese company Toyama, a subsidiary of Fuji Film, as reported by Furuta in 2002 (Furuta et al., 2002). It was approved in Japan in 2014 as a substitute option for resistant influenza infection and has since been approved in several countries and is indicated for the treatment of patients with mild to moderate COVID-19 disease (Agrawal et al. 2020). Favipiravir is an RNA-dependent RNA polymerase inhibitor. It is activated in cells in its phosphoribosylated form (Favipiravir-RTP) and inhibits viral RNA polymerase activity (Allen et al., 2020).

For this purpose, molecular coupling of three SARS-CoV-2 proteins with three active ingredients previously reported to be active in vitro was performed (Şahin et al., 2022). The insertion results of these three compounds were compared with three FDA-Approved Drugs currently in use in COVID 19, namely Remdesivir, Favipiravir and Litonavir.

Material and Method

All docking experiments were performed using Autodock 4.2 (Morris et al., 2014) program to examine protein-ligand interactions at the active site and estimate binding affinity scores. Preparation of proteins and ligands for molecular docking was done using MGLTools. Water molecules were removed, hydrogen added, torsional angles verified, and Kollman charges added. The ligand binding site was then used for all the downloaded proteins to identify the active site of the protein. The receiver grid generation workflow was used to define a grid (box) around the ligand to hold all functional residues in the grid (Table 1).

The Lamarckian Genetic Algorithm (LA) protocol was applied to perform molecular insertion. Pole interactions, Van der Waals forces, and interactions between other non-covalent protein and coupled ligand were estimated using the Autodock calculation method. All protein constructs used in splicing experiments were obtained from the Research Collaboration for Structural Bioinformatics Protein Data Bank (PDB). Ligand structure XRD results CIF file was converted to SDF file using OPENBABELGUI, SDF file was converted to the most stable structure, PDB format, by energy minimization with AVAGADRO program. Ligand and protein molecules were converted to suitable readable file formats (pdbqt) using AutoDockTools 1.5.6. All other software parameters were default values and free spin of all ligands present in the ligand was allowed when the receptor was solid. The generated output files were converted to protein-ligand complex, which was analyzed using BioVia Discovery Studio Software.

Result and Discussion

As a part of the research aimed at synthesis of novel tetrols we have prepared halogenated bicyclo[4.2.0] inositols and a cyclic sulfate derivative from *syn*-bisepoxide (5) (Figure 2) (Karanfil et al., 2020). Starting from the commercially available cyclooctatetraene (COT), synthesis of *syn*-bisepoxide easily carried out using literature protocols (Adam & Balci, 1980). The reaction of the bisepoxide (5) with acidified acetic anhydride gave a mixture of 3 tetraacetate isomers (6, 7 and 8) and an unexpected cyclic sulfate (9) derivative (Karanfil et al., 2020). Separation of the tetraacetates and removal of the acetate functionalities with ammonia gave the expected novel halogenated bicyclo[4.2.0] inositols (10) resembling dihydrocondurotol-A, -B, and -F structures (Figure 3).

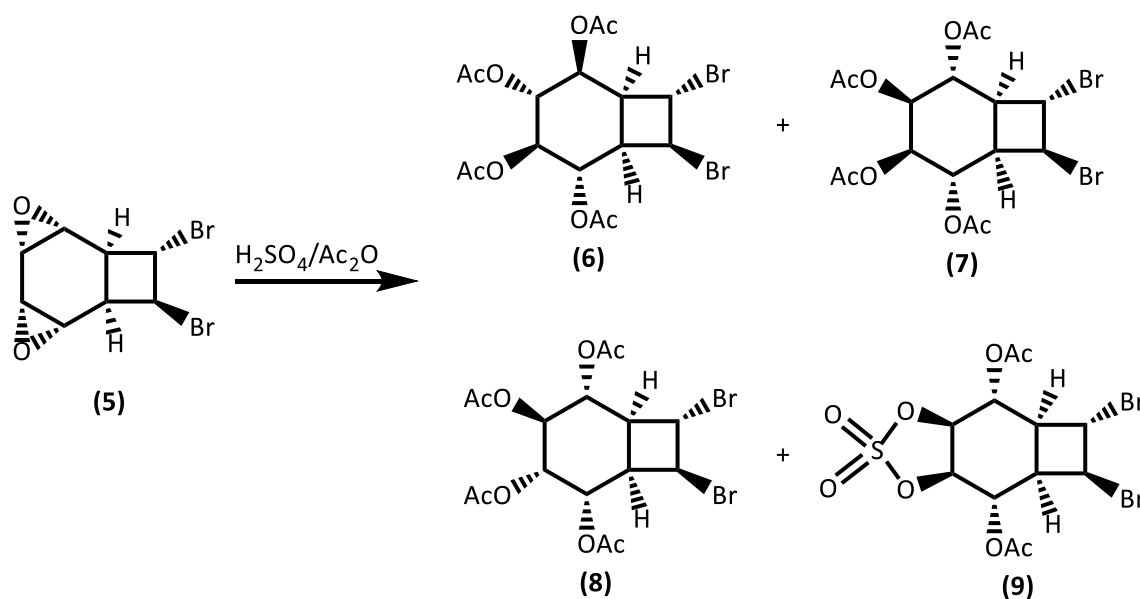


Figure 2. Ring-opening Reaction of Bisepoxide 5

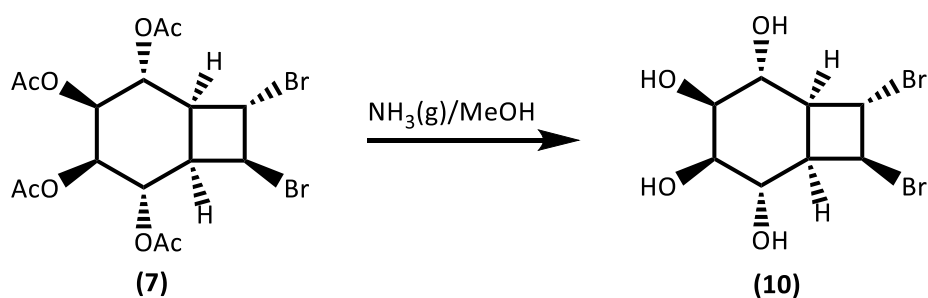


Figure 3. Ammonolysis of Tetraacetate 7

In this study a docking study of halogenated bicyclo[4.2.0] inositol derivatives (6, 9, and 10) was performed against the reference molecules, FDA-Approved Drug Remdesivir, Lopinavir and Favipiravir with the therapeutic target proteins of SARS-CoV-2, i.e., SGp, Mpro, and Endoribonuclease Nsp15/NendoU, used in patients intubated for COVID-19 treatment.

The binding energies of the cyclic sulfate and the FDA-Approved Remdesivir, Lopinavir, Favipiravir with the therapeutic target proteins of SARS-CoV-2, i.e., SGp, Mpro, and Endoribonuclease Nsp15/NendoU are summarized in Table 2.

Table 1. Details of Protein Targets, 3D Structures and Their Active Sites

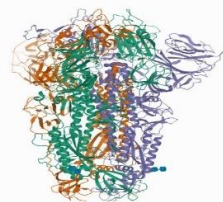
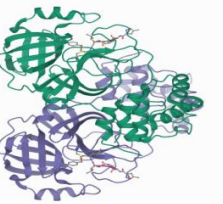
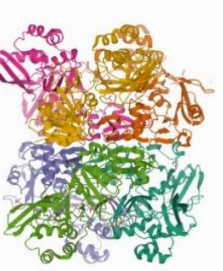
S.No	PDB Protein Code	Protein Name	3-D Structure	Interactions with Selected Amino Acids at Binding Sites
1	6ZB5	CoV-2 Spike protein		Cys336, Phe338, Val341, Phe342, Cys361, Phe374, Phe377, Phe392, Arg408, Gln409, Cys432, Trp436, Phe515.
2	6LU7	COVID-19 main protease		Thr24, Thr25, Thr26, His41, Met49, Tyr54, Leu141, Asn142, Gly143, Ser144, Cys145, His164, Met165, Glu166, Leu167, Pro168, His172, Asp187, Arg188, Gln189, Thr190, Ala191, Gln192.
3	6VWW	NSP15 Endoribonuclease SARS CoV2		His235, His250, Lys290, Ser294, Thr341, Tyr343.

Table 2. Comparative Dock Score of Ligands with Therapeutic Target Proteins of COVID-19 (kcalmol⁻¹)

Ligand	SARS CoV-2 Spike Protein, Closed Conformation, C3 Symmetry	COVID-19 Mpro in Complex with the Inhibitor N3	Crystal Structure of NSP15 Endoribonuclease from SARS CoV-2
Cyclic Sulfate (9)	-7,29	-7,33	-7,29
Acetate (6)	-6,44	-7,45	-6,54
Tetrol (10)	-4,89	-5,69	-5,0
Control Drugs			
Lopinavir	-	-12,05	-
Remdesivir	-5,36	-	-
Favipiravir	-	-	-4,46

Remdesivir, pi-alkyl interaction with Lys378, pi-pi stacked interaction with Tyr365, pi-lone pair interaction with Phe377, pi-donor hydrogen bond interaction Phe377, conventional hydrogen bond with Phe374 and Phe377(2) and Vdw (Van der Waals) interactions with Tyr369, Ala372, Ser373, Ser375, Thr376, Pro384 and Leu387 showed binding affinity to SARS CoV-2 spike protein, closed conformation, C3 symmetry chain C residues active site with binding energy of $-5.36 \text{ kcal mol}^{-1}$. Cyclic Sulfate (9), pi-alkyl interaction with Phe374 and Tyr369, pi-sulfur interaction with Phe377, carbon hydrogen bond with Ser373, conventional hydrogen bond with Phe374(2) and Tyr369 and Vdw interactions with Tyr365, Leu368, Ala372 and Thr376 showed binding affinity to SARS CoV-2 spike protein, closed conformation, C3 symmetry chain C residues active site with binding energy of $-7.29 \text{ kcal mol}^{-1}$. Acetate (6) pi-alkyl interaction with Tyr369 and Phe374(2), alkyl interaction with Leu368, conventional hydrogen bond with Phe374 and Tyr369 and Vdw interactions with Tyr365, Ala372, Ser373, Phe377, Pro384 and Leu387 showed binding affinity to SARS-CoV-2 spike protein, closed conformation, C3 symmetry chain C residues active site with binding energy of $-6.44 \text{ kcal mol}^{-1}$. Tetrol (10), alkyl interaction with Val407, conventional hydrogen bond with Gly404, Arg408 and Asp405(2) and Vdw interactions with Glu406, Val503, Gly504 and Gly508 showed binding affinity to SARS CoV-2 spike protein, closed conformation, C3 symmetry chain C residues active site with binding energy of $-4.89 \text{ kcal mol}^{-1}$ (Figure 4).

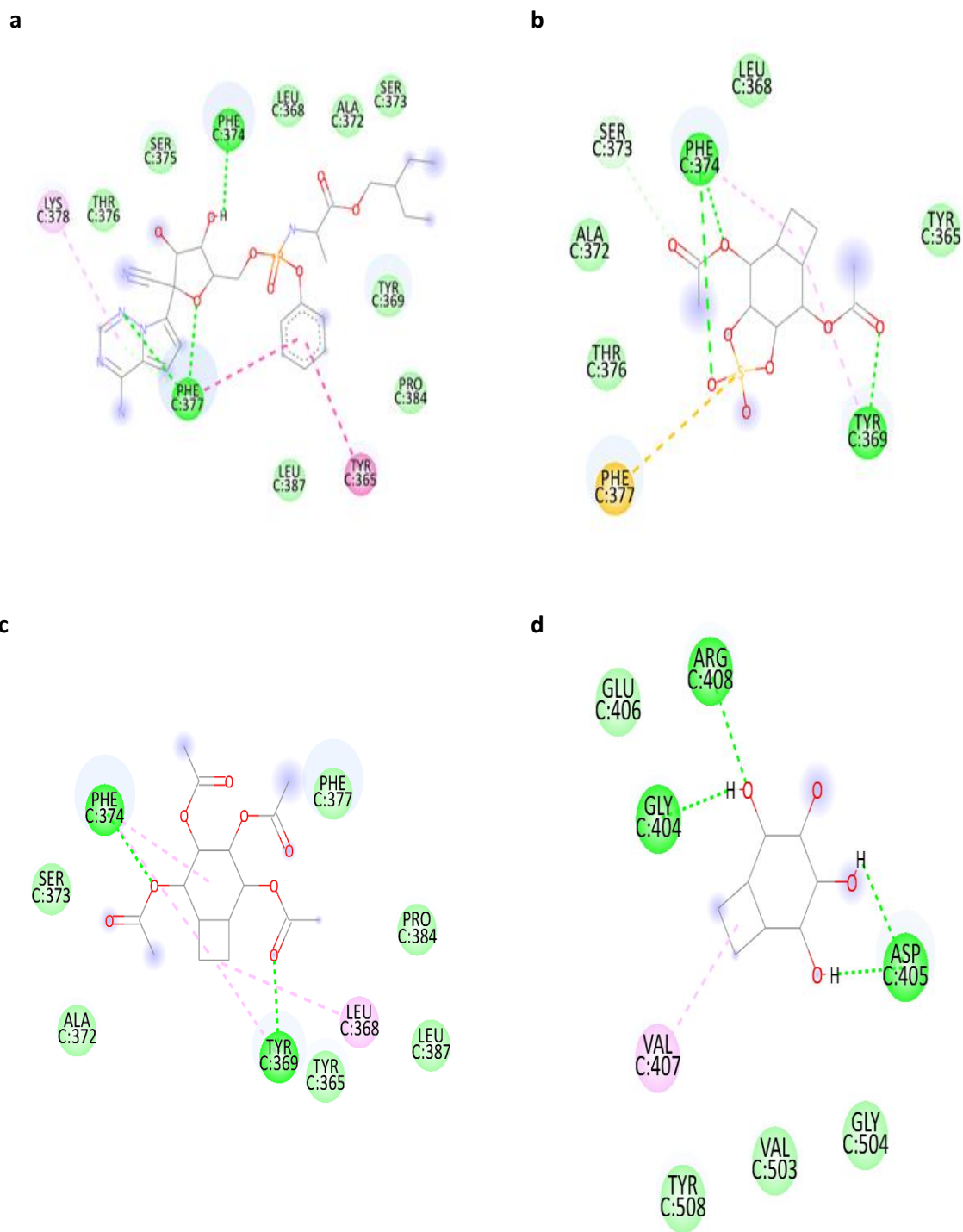


Figure 4. Remdesivir (a), Cyclic Sulfate (b), Acetate (c) and Tetrol (d) Docked in the SARS-CoV-2 Spike Protein, Closed Conformation, C3 Symmetry (PDB ID: 6zb5) with 2D Animated Pose Showing Non-Covalent Interactions between Cyclic Sulfate and SGp

Lopinavir, COVID-19 Mpro in complex with the inhibitor N3 A chain, alkyl interaction with Cys145, Pro168, pi-sigma interaction with His41, pi-alkyl interaction with Met49, Met165(2), Pro168, Ala191, pi-cation interaction with His41, pi-pi stacking interaction with His41, pi-pi T-shaped interaction with His41, amide-pi stacked interaction with Asp187, Thr190, carbon-hydrogen bond with Glu166, pi-donor hydrogen bond with Cys145, Glu166, and Vdw interactions with Tyr54, Asn142, Gly143, Ser144, His164, Leu167, Arg188, Gln189 and Gln192 showed binding affinity to COVID-19 Mpro in complex with the inhibitor N3 chain A residues active site with binding energy of $-12.05 \text{ kcal mol}^{-1}$. Cyclic Sulfate (9), COVID-19 Mpro in complex with the inhibitor N3 A chain, carbon-hydrogen bond with Leu141(2), Asn142(2), alkyl interaction with Cys145, pi-alkyl interaction with His41, pi-sulfur interaction with His163, conventional *H*-bond with Phe140, Gly143, His163, Glu166 and Vdw interactions with Ser144, His164, His172 and Gln189 showed binding affinity to COVID-19 Mpro in complex with the inhibitor N3 chain A residues active site with binding energy of $-7,33 \text{ kcal mol}^{-1}$. Acetate (6), COVID-19 Mpro in complex with the inhibitor N3 A chain, carbon-hydrogen bond with His164, conventional hydrogen bond with His41, Gly143, Ser144, Cys145(3), Glu166 and Vdw interactions with Leu27, Met49, Phe140, Leu141, Asn142, Met165, His172, His172 and Gln189 showed binding affinity to COVID-19 Mpro in complex with the inhibitor N3 chain A residues active site with binding energy of $-7,45 \text{ kcal mol}^{-1}$. Tetrol (10), COVID-19 Mpro in complex with the inhibitor N3 A chain, conventional hydrogen bond with His164, Glu166, Gln189(2) and Vdw interactions with His41, Met49, Cys145, His163 and Met165 showed binding affinity to COVID-19 Mpro in complex with the inhibitor N3 chain A residues active site with binding energy of $-5.69 \text{ kcal mol}^{-1}$ (Figure 5).

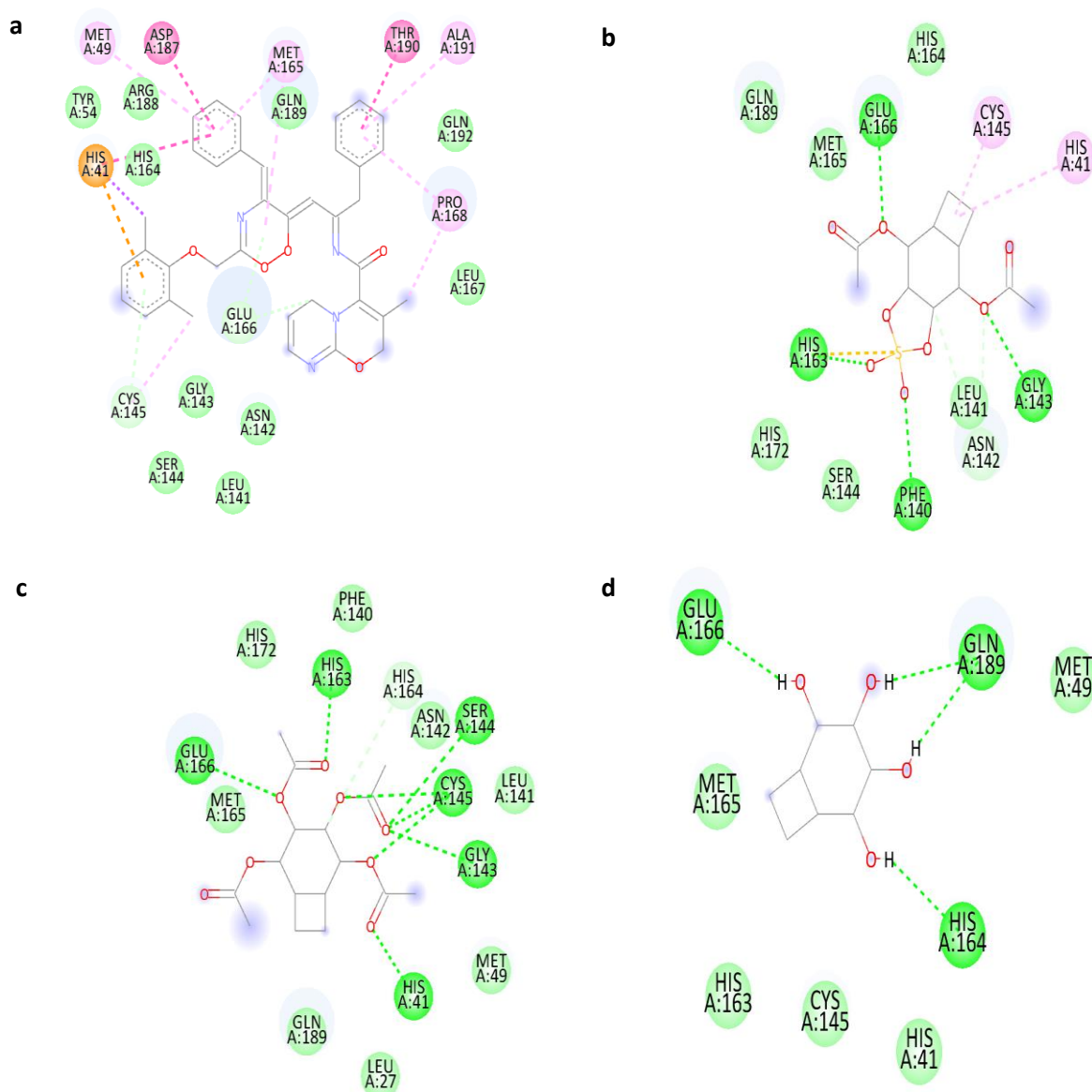


Figure 5. Lopinavir (a), Cyclic Sulfate (b), Acetate (c) and Tetrol (d) Docked in the COVID-19 Mpro in Complex with the Inhibitor N3 (PDB ID: 6LU7) with 2D Animated Pose Showing Non-Covalent Interactions between Cyclic Sulfate and Mpro

Favipiravir, Crystal Structure of NSP15 Endoribonuclease from SARS CoV-2 A conventional hydrogen with His250, Lys290, Ser294(2), carbon-hydrogen bond with His250, pi-alkyl interaction with Val292, pi-pi stacked interaction with Tyr343 and Vdw interactions with Gly248, Cys293, Lys345 and Leu346 showed binding affinity to Crystal Structure of NSP15 Endoribonuclease from SARS-CoV-2 A residues active site with binding energy of $-4.46 \text{ kcal mol}^{-1}$. Cyclic Sulfate (9), Crystal Structure of NSP15 Endoribonuclease from SARS-CoV-2 A conventional hydrogen with His235, Gly248, Lys290(2), Thr341, carbon-hydrogen bond with His250, pi-sulfur interaction with His235, His250, pi-alkyl interaction with Tyr343 and Vdw interactions with Gly247, Val292, Cys293, Ser294, Trp333, Pro344, Lys345 showed binding affinity to Crystal Structure of NSP15 Endoribonuclease from SARS-CoV-2 A residues active site with binding energy of $-7,29 \text{ kcal mol}^{-1}$. Acetate (6), Crystal Structure of NSP15 Endoribonuclease from SARS-CoV-2 A conventional hydrogen with His250, Lys290, Cys291, Val292, Ser294, pi-sigma interaction with Tyr343, alkyl interaction with Lys290, Val292(2), Leu346 and Vdw interactions with Gln245, Gly248, Val292, Cys293, Thr341 and Pro344 showed binding affinity to Crystal Structure of NSP15 Endoribonuclease from SARS-CoV-2 A residues active site with binding energy of $-6.54 \text{ kcal mol}^{-1}$

¹. Tetrol (10), Crystal Structure of NSP15 Endoribonuclease from SARS-CoV-2 A conventional hydrogen with Lys290, Val292, carbon-hydrogen bond with His250, pi-alkyl Tyr343 interaction with His235, His250, alkyl interaction with Leu346 and Vdw interactions with Cys293, Ser294, Pro344, Lys345 showed binding affinity to Crystal Structure of NSP15 Endoribonuclease from SARS-CoV-2 A residues active site with binding energy of $-5.0 \text{ kcal mol}^{-1}$ (Figure 6).

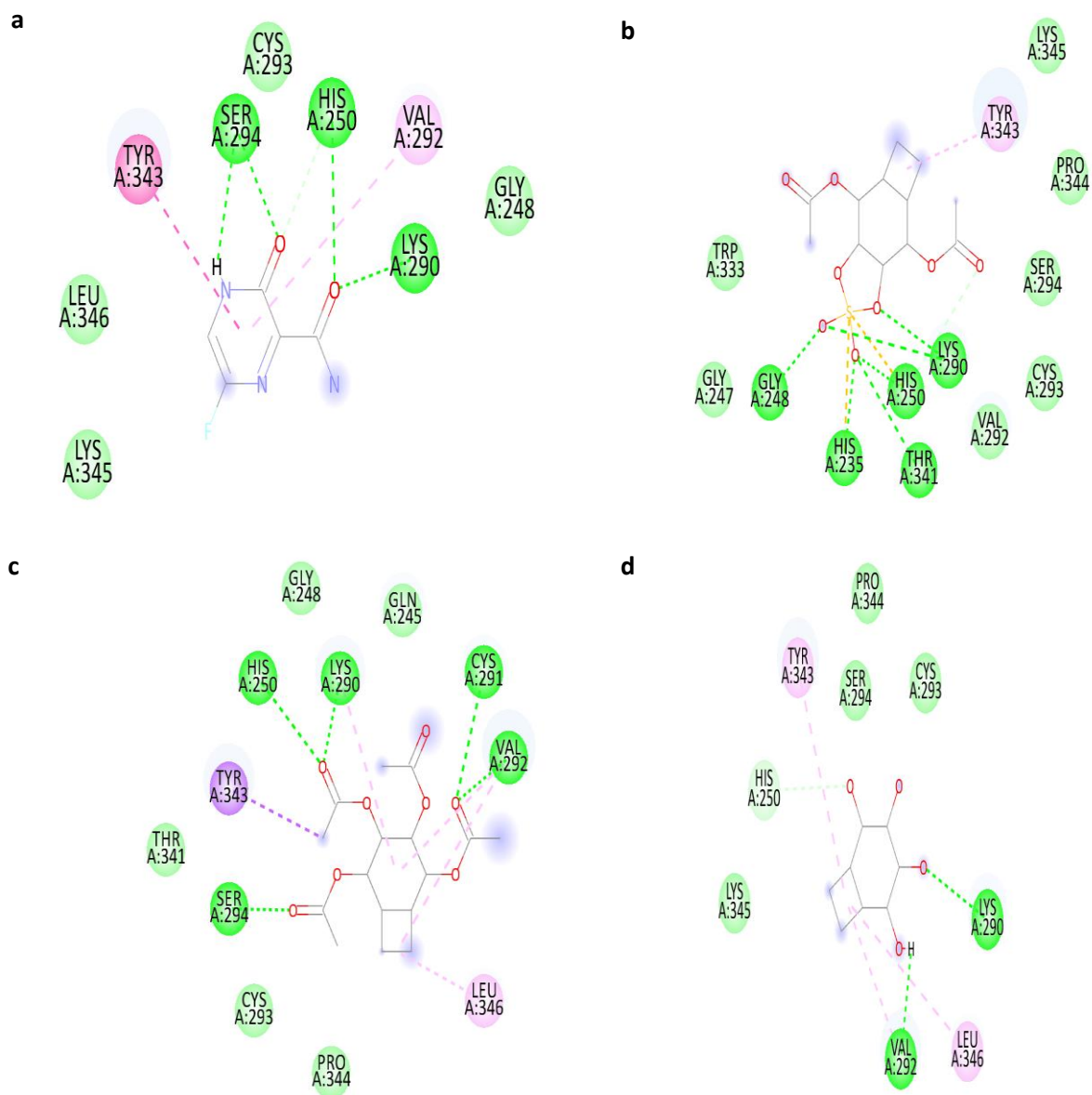


Figure 6. Favipiravir (a), Cyclic Sulfate (b), Acetate (c) and Tetrol (d) Docked in the Crystal Structure of NSP15 Endoribonuclease from SARS-CoV-2 (PDB ID: 6VWW) with 2D Animated Pose Showing Non-Covalent Interactions between Cyclic Sulfate and Endoribonuclease Nsp15/NendoU

In this article, we examined the potential benefit of halogenated bicyclo[4.2.0] inositols (4), whose inhibitory effects were evaluated, in reducing the inflammatory response on SARS-CoV-2 infection. The management of the disease is mostly supportive, and respiratory failure from acute respiratory distress syndrome is the leading cause of death in a significant proportion of affected patients. Considering the knowledge of myo-inositol (2), a polyol currently used to treat Neonatal Respiratory Distress Syndrome, we investigated the potential utility of newly synthesized halogenated bicyclo[4.2.0]inositols (4) (Karanfil et al 2020) in reducing the inflammatory response on SARS-CoV-2 infection. Preliminary data indicate that the dramatic increase in IL-6 and the ensuing cytokine release

syndrome may explain the development of fatal interstitial pneumonia. Inhibition of IL-6 by blocking its specific receptor with monoclonal antibodies has been advocated as a promising intervention. Myo-Inositol (2) has been proven to reduce IL-6 levels in a few conditions and alleviate the inflammatory cascade while devoid of any major side effects. Therefore, it is tempting to think that inositol may be useful in managing the dire effects of SARS-CoV-2 infection. SARS-CoV-2 infection or spike protein expression in human epithelial cells inhibits ACE2 expression and promotes IL-6/soluble IL-6R release. ACE2 expression is inhibited upon SARS-CoV-2 infection or spike gene transfection. Our crystal structure and docking data suggest that the ligand (cyclic sulfate 9) can bind to the substrate binding pocket of SARS-CoV-2 SGp at a high level. These interactions can collectively prevent SGp-RBD from binding to the receptor ACE2. Lopinavir, a vRNA polymerase inhibitor, has also shown the possibility of having inhibition of the COVID-19 major protease enzyme; this enzyme is responsible for the replication of the virus in the living body. To reach this conclusion, we have completed the journey of ligands insertion analysis with the COVID-19 major protease PDB ID: 6lu7. Initially, the Lopinavir control drug and 3 small drugs with the possibility of protease inhibition of the virus were placed, the results were observed and analyzed. Further residue analysis indicated that acetate (6) and cyclic sulfate (9) may have protease inhibition possibilities for the interruption of viral replication as amino acids of the binding pocket for acetate (6). Cyclic sulfate (9) was like the reference molecule N3 complexes in the 3D structure of the COVID-19 major protease 6lu7. This strongly supports the hypothesis that the development of a single antiviral agent targeting Mpro, or such an agent used in combination with other potential treatments, could provide an effective first line of defense against all coronavirus-related diseases. These results primarily showed only possibilities, but clinical studies are still needed to confirm the findings.

Conclusion

Our results reveal that cyclic sulfate (9) may inhibit SARS-CoV-2 target proteins (SGp, nsp15 and Mpro) in the least energy conformation. We have identified cyclic sulfate (9) as an important halogenated bicyclo[4.2.0] inositol derivative. However, the human ACE2 receptor was found to interact best with halogenated bicyclo[4.2.0]inositol acetate (6). After conducting this study, we propose new cyclic sulfate (9) and acetate (6) (separately or in combination) as important halogenated bicyclo[4.2.0]inositol compounds effective against SARS-CoV-2. The current work could be very helpful in stopping the further growth of the COVID-19 pandemic.

Acknowledgement

The authors are indebted to Ordu University Scientific Research Projects Coordination Unit (ODU/BAP, Grant No: AR-1659) and Ataturk University Scientific Research Projects Coordination Unit (BAP, Project No. 2013/77) for financial support of this work.

Authors' Contributions

Ebrar Nur Şahin, molecular docking, preparation of the manuscript. *Abdullah Karanfil*, synthesis and characterization compounds, preparation of the manuscript. *Ertan Şahin*, molecular docking, preparation of the manuscript and wrote the manuscript. *Latif Kelebekli*, designed the study, critically evaluated the results, and wrote the manuscript. All authors read and approved the final version of the manuscript.

Ethics

There are no ethical issues related to the publication of this article.

Conflicts of Interest

The authors declare that they have no known competing financial interests or personal relationships that could have appeared to influence the work reported in this paper.

ORCID

Ebrar Nur Şahin  <https://orcid.org/0000-0002-1222-1500>

Abdullah Karanfil  <https://orcid.org/0000-0003-2948-4216>

Ertan Şahin  <https://orcid.org/0000-0002-6311-8917>

Latif Kelebekli  <https://orcid.org/0000-0002-6242-2589>

References

- Adam, W., & Balci, M. (1980). Cyclic polyepoxides: Synthetic, structural and biological aspects. *Tetrahedron*, 36(7), 833-858. [https://doi.org/10.1016/0040-4020\(80\)80034-2](https://doi.org/10.1016/0040-4020(80)80034-2)
- Aksu, A., Akincioglu, H., Gulcin, İ., & Kelebekli, L. (2021). Concise syntheses and some biological activities of DL-2,5-di-O-methyl-chiro-inositol, DL-1,4-di-O-methyl-scylo-inositol, and DL-1,6-dibromo-1,6-dideoxy-2,5-di-O-methyl-chiroinositol. *Archiv der Pharmazie*, 354, e2000254. <https://doi.org/10.1002/ardp.202000254>
- Agostini, M. L., Andres, E. L., Sims, A. C., Graham, R. L., Sheahan, T. P., Lu, X., Smith, E. C., Case, J. B., Feng, J. Y., Jordan, R., Ray, A. S., Cihlar, T., Siegel, D., Mackman, R. L., Clarke, M. O., Baric, R. S., & Denison, M. R. (2018). Coronavirus susceptibility to the antiviral remdesivir (GS-5734) is mediated by the viral polymerase and the proofreading exoribonuclease. *mBio*, 9(2), e00221-18. <https://doi.org/10.1128/mBio.00221-18>
- Agrawal, U., Raju, R., & Udwardia, Z. F. (2020). Favipiravir: A new and emerging antiviral option in COVID-19. *Medical Journal Armed Forces India*, 76(4), 370–376. <https://doi.org/10.1016/j.mjafi.2020.08.004>
- Allen, C. N. S., Arjona, S. P., Santerre, M., & Sawaya, B. E. (2020). Potential use of RNA-dependent RNA polymerase (RdRp) inhibitors against SARS-CoV2 infection. *All Life*, 13(1), 608–614. <https://doi.org/10.1080/26895293.2020.1835741>
- Arouche, T. D. S., Martins, A. Y., Ramalho, T. C., Júnior, R. N. C., Costa, F. L. P., Filho, T. S. A., & Neto, A. M. J. C. (2021). Molecular Docking of Azithromycin, Ritonavir, Lopinavir, Oseltamivir, Ivermectin and Heparin Interacting with Coronavirus Disease 2019 Main and Severe Acute Respiratory Syndrome Coronavirus-2 3C-Like Proteases. *Journal of Nanoscience and Nanotechnology*, 21(4), 2075-2089. <https://doi.org/10.1166/jnn.2021.19029>
- Bizzarri, M., Laganà, A. S., Aragona, D., & Unfer, V. (2020). Inositol and pulmonary function. Could myo-inositol treatment downregulate inflammation and cytokine release syndrome in SARS-CoV-2? *European Review for Medical and Pharmacological Sciences*, 24(6), 3426-3432. https://doi.org/10.26355/eurev_202003_20715
- Brown, A. J., Won, J. J., Graham, R. L., Dinnon, K. H., Sims, A. C., Feng, J. Y., Cihlar, T., Denison, M. R., Baric, R. S., & Sheahan, T. P. (2019). Broad spectrum antiviral remdesivir inhibits human endemic and zoonotic deltacoronaviruses with a highly divergent RNA dependent RNA polymerase. *Antiviral Research*, 169, 104541. <https://doi.org/10.1016/j.antiviral.2019.104541>
- de Wit, E., Feldmann, F., Cronin, J., Jordan, R., Okumura, A., Thomas, T., Scott, D., Cihlar, T., & Feldmann, H. (2020). Prophylactic and therapeutic remdesivir (GS-5734) treatment in the rhesus macaque model of MERS-CoV infection. *Proceedings of the National Academy of Sciences*, 117(12), 6771-6776. <https://doi.org/10.1073/pnas.1922083117>

- de Wit, E., Rasmussen, A. L., Falzarano, D., Bushmaker, T., Feldmann, F., Brining, D. L., Fischer, E. R., Martellaro, C., Okumura, A., Chang, J., Scott, D., Benecke, A. G., Katze, M. G., Feldmann, H., & Munster, V. J. (2013). Middle East respiratory syndrome coronavirus (MERS-CoV) causes transient lower respiratory tract infection in rhesus macaques. *Proceedings of the National Academy of Sciences*, 110(41), 16598-16603. <https://doi.org/10.1073/pnas.1310744110>
- Espinola, M. S. B., Bertelli, M., Bizzarri, M., Unfer, V., Laganà, A. S., Visconti, B., & Aragona, C. (2021). Inositol and vitamin D may naturally protect human reproduction and women undergoing assisted reproduction from Covid-19 risk. *Journal of Reproductive Immunology*, 144, 103271. <https://doi.org/10.1016/j.jri.2021.103271>
- Food, U., & Administration, D. (2020). *Fact Sheet for Health Care Providers Emergency Use Authorization (EUA) of Veklury® (remdesivir)*. <https://www.fda.gov/media/137566/download>
- Furuta, Y., Takahashi, K., Fukuda, Y., Kuno, M., Kamiyama, T., Kozaki, K., Nomura, N., Egawa, H., Minami, S., Watanabe, Y., Narita, H., & Shiraki, K. (2002). In vitro and in vivo activities of anti-influenza virus compound T-705. *Antimicrobial Agents and Chemotherapy*, 46(4), 977-981. <https://doi.org/10.1128/AAC.46.4.977-981.2002>
- Kamenov, Z., & Gateva, A. (2020). Inositols in PCOS. *Molecules*, 25(23), 5566. <https://doi.org/10.3390/molecules25235566>
- Karanfil, A., Şahin, E., & Kelebekli, L. (2020). Synthesis of novel tetrols from syn-bisepoxide: Preparation of halogenated bicyclo[4.2.0] inositols. *Tetrahedron*, 76(11), 131000. <https://doi.org/10.1016/j.tet.2020.131000>
- Kelebekli, L., Kara, Y., & Balci, M. (2005). Stereospecific synthesis of a new class of compounds: bis-homoconduritol-A, -D, and-F. *Carbohydrate Research*, 340(12), 1940-1948. <https://doi.org/10.1016/j.carres.2005.05.021>
- Kelebekli, L., & Kaplan, D. (2017). Stereospecific synthesis of novel methyl-substituted mono- and dimethoxy Conduritols. *Tetrahedron*, 73, 8-13. <http://dx.doi.org/10.1016/j.tet.2016.11.042>
- Kelebekli, L., & Atlı, İ. (2019). Stereoselective synthesis of a new methyl-substituted inositol Derivative, *Tetrahedron*, 75, 130531. <https://doi.org/10.1016/j.tet.2019.130531>
- Lagana, A. S., Unfer, V., Garzon, S., & Mariano Bizzarri, M. (2020). Role of inositol to improve surfactant functions and reduce IL-6 levels: A potential adjuvant strategy for SARS-CoV-2 pneumonia? *Medical Hypotheses*, 144, 110262. <https://doi.org/10.1016/j.mehy.2020.110262>
- López, M. D., Cobo, J., & Noguera, M. (2008). Building Bicyclic Polyhydroxylated Alkaloids: An Overview from 1995 to the Present. *Current Organic Chemistry*, 12(9), 718-750. <https://doi.org/10.2174/138527208784567197>
- Goodsell D. S, Morris G. M, Olson A. J. (1996). Automated docking of flexible ligands: applications of AutoDock. *J. Mol. Recognit*, 9(1), 1-5. [https://doi.org/10.1002/\(SICI\)1099-1352\(199601\)9:1<1::AID-JMR241>3.0.CO;2-6](https://doi.org/10.1002/(SICI)1099-1352(199601)9:1<1::AID-JMR241>3.0.CO;2-6)
- Rafi, M. O., Bhattacharje, G., Al-Khafaji, K., Taskin-Tok, T., Alfasane, M. A., Das, A. K., Parvez, M. A. K., & Rahman, M. S. (2020). Combination of QSAR, molecular docking, molecular dynamic simulation and MM-PBSA: analogues of lopinavir and favipiravir as potential drug candidates against COVID-19. *Journal of Biomolecular Structure and Dynamics*, 30, 1-20. <https://doi.org/10.1080/07391102.2020.1850355>

- Rubin, D., Chan-Tack, K., Farley, J., & Sherwat, A. (2020). FDA Approval of Remdesivir — A Step in the Right Direction. *New England Journal of Medicine*, 383, 2598–2600. <https://doi.org/10.1056/NEJMp2032369>
- Sheahan, T. P., Sims, A. C., Graham, R. L., Menachery, V. D., Gralinski, L. E., Case, J. B., Leist, S. R., Pyrc, K., Feng, J. Y., Trantcheva, I., Bannister, R., Park, Y., Babusis, D., Clarke, M. O., Mackman, R.L., Spahn, J. E., Palmiotti, C. A., Siegel, D., Ray, A. S., & Baric, R.S. (2017). Broad-spectrum antiviral GS-5734 inhibits both epidemic and zoonotic coronaviruses. *Science Translational Medicine*, 9(396), eaal3653. <https://doi.org/10.1126/scitranslmed.aal3653>
- Sun, Y., Zhang, G., Hawkes, C. A., Shaw, J. E., McLaurin, J. A., & Nitz, M. (2008). Synthesis of scyllo-inositol derivatives and their effects on amyloid beta peptide aggregation. *Bioorganic & Medicinal Chemistry*, 16(15), 7177-7184. <https://doi.org/10.1016/j.bmc.2008.06.045>
- Şahin, E. N., Karanfil, A., Ayvaz, M. Ç., Şahin, E., & Kelebekli, L. (2022). Structural analysis of halogenated bicyclo[4.2.0] inositols, biological activities and molecular docking studies. *Journal of Molecular Structure*, 1248, 131357. <https://doi.org/10.1016/J.MOLSTRUC.2021.131357>
- Wang, M., Cao, R., Zhang, L., Yang, X., Liu, J., Xu, M., Shi, Z., Hu, Z., Zhong, W., & Xiao, G. (2020). Remdesivir and chloroquine effectively inhibit the recently emerged novel coronavirus (2019-nCoV) in vitro. *Cell Research*, 30, 269–271. <https://doi.org/10.1038/s41422-020-0282-0>
- Wang, N., Hang, L-H., & Ye, X-S. (2010). A new synthetic access to bicyclic polyhydroxylated alkaloid analogues from pyranosides. *Organic & Biomolecular Chemistry*, 11(8), 2639-2649. <https://doi.org/10.1039/B923180C>
- Wu, R., Wang, L., Kuo, H-C. D., Shannar, A., Peter, R., Chou, P. J., Li, S., Hudlikar, R., Liu, X., Liu, Z., Poiani, G. J., Amorosa, L., Brunetti, L., & Kong, A-N. (2020). An Update on Current Therapeutic Drugs Treating COVID-19. *Current Pharmacology Reports*, 6, 56-70. <https://doi.org/10.1007/s40495-020-00216-7>
- Zanardi, F., Battistini, L., Marzocchi, L., Acquotti, D., Rassu, G., Pinna, L., Auzzas, L., Zambrano, V., & Casiraghi, G. (2002). Synthesis of a Small Repertoire of Non-Racemic 5a-Carbahexopyranoses and 1-Thio-5a-carbahexopyranoses. *European Journal of Organic Chemistry*, 2002(12), 1956-1964. [https://doi.org/10.1002/1099-0690\(200206\)2002:12<1956::AID-EJOC1956>3.0.CO;2-Y](https://doi.org/10.1002/1099-0690(200206)2002:12<1956::AID-EJOC1956>3.0.CO;2-Y)